Salinity Adjustments in the Presence of Temperature Data Assimilation

ALBERTO TROCCOLI,* MAGDALENA ALONSO BALMASEDA, JOACHIM SEGSCHNEIDER,[+]
JEROME VIALARD, AND DAVID L. T. ANDERSON,

European Centre for Medium-Range Weather Forecasts, Reading, United Kingdom

KEITH HAINES,[#]

Meteorology Department, Edinburgh University, Edinburgh, United Kingdom

TIM STOCKDALE, AND FREDERIC VITART,

European Centre for Medium-Range Weather Forecasts, Reading, United Kingdom

ALAN D. FOX

Meteorology Department, Edinburgh University, Edinburgh, United Kingdom

(Manuscript received 4 April 2001, in final form 2 July 2001)

ABSTRACT

This paper is an evaluation of the role of salinity in the framework of temperature data assimilation in a global ocean model that is used to initialize seasonal climate forecasts. It is shown that the univariate assimilation of temperature profiles, without attempting to correct salinity, can induce first-order errors in the subsurface temperature and salinity fields. A recently developed scheme by A. Troccoli and K. Haines is used to improve the salinity field. In this scheme, salinity increments are derived from the observed temperature, by using the model temperature and salinity profiles, assuming that the temperature–salinity relationship in the model profiles is preserved. In addition, the temperature and salinity fields are matched below the observed temperature profile by vertically displacing the original model profiles.

Two data assimilation experiments were performed for the 6-yr period 1993–98. These show that the salinity scheme is effective at maintaining the haline and thermal structures at and below thermocline level, especially in tropical regions, by avoiding spurious convection. In addition to improvements in the mean state, the scheme allows more temporal variability than simply controlling the salinity field by relaxation to climatological data. Some comparisons with sparse salinity observations are also made, which suggest that the subsurface salinity variability in the western Pacific is better reproduced in the experiment in which the salinity scheme is used. The salinity analyses might be improved further by use of altimeter sea level or sea surface salinity observations from satellite.

1. Introduction

A currently used strategy to produce ocean analyses for seasonal forecast purposes is to force an ocean model with recent history of wind stress, heat fluxes, and precipitation minus evaporation fields, and then use the analyzed ocean state as initial conditions in a coupled ocean–atmosphere model. It is mainly the subsurface structure of the temperature fields that provides predictive skill on the timescale of a few months. The analyzed ocean states are not perfect, however, as both forcing fields and ocean models contain errors. Ocean temperature data assimilation has proven to be capable of improving the simulated upper ocean temperature structure in such a way as to be beneficial for seasonal climate forecasting (e.g., Alves et al. 1999; Ji et al. 1998; Fischer et al. 1997; Rosati et al. 1997). The seasonal forecasting system at the European Centre for Medium-Range Weather Forecasts (ECMWF) uses an ocean analysis in which in situ temperature data have been assimilated.

Not much attention has been given to salinity in the context of temperature data assimilation for seasonal climate forecasts. Hitherto, the most common approach has been to leave the salinity field unmodified when updating the temperature field. This is partly because

* Current affiliation: NASA Interannual-to-Seasonal Prediction Project, NASA/GEST, Greenbelt, Maryland.
[+] Current affiliation: ISAO-CNR, Bologna, Italy.
[#] Current affiliation: Environmental Systems Science Centre, Reading University, Reading, United Kingdom.

Corresponding author address: Dr. Alberto Troccoli, NSIPP, NASA/GEST, Code 971, Bldg. 33, Greenbelt, MD 20771.
E-mail: troccoli@janus.gsfc.nasa.gov

subsurface salinity observations available in near–real time are very sparse, and partly because the salinity field was thought to be of less importance for the density in the upper tropical ocean. However we will show that not modifying salinity when updating temperature may lead to the generation of artificial and unrealistic water masses which corrupt the model state. We show that this can cause serious errors not only in salinity, but also in the temperature field.

As pointed out by Cooper over a decade ago (Cooper 1988), salinity variability also sometimes plays an important role in determining the three-dimensional density structure even in tropical regions. Recently, observations in the western equatorial Pacific have revealed large interannual variations of salinity at subsurface levels (Kessler 1999; Ji et al. 2000). The physical causes for the observed anomalies are not fully explored yet, and it is also unclear to what extent the ocean analyses at ECMWF, in which salinity is treated as a prognostic tracer, can reproduce the observed changes.

Recently, several different attempts have been made to infer salinity when temperature is the only subsurface data available. Some of the proposed methods make use of Empirical Orthogonal Functions (EOFs) to decompose the vertical structure of temperature (T) and salinity (S) profiles and determine relationships between them, as observed over limited regions and periods. The EOFs thus obtained are used to derive salinity from T when direct observations of S are not available. For example, Vossepoel et al. (1999) used 9000 T and S profiles in the equatorial Pacific for the period 1975–96 (i.e., an average of about 3 observations per year in a $1°$ by $1°$ region). The EOFs of the data provide a correction to a first guess, which is obtained from a climatological $T–S$ relation, so as to improve the S variability. However, the representativeness of the EOFs depends on the availability of T and S observations. Because of the sparsity of S data, it is difficult to extend these results to regions outside the tropical Pacific. Furthermore, the fact that EOFs can only represent structures that are present in the training data may prevent reconstruction of S profiles that have not been observed in the past.

An approach that overcomes some of the limitations of the methods described above has been proposed by Troccoli and Haines (1999, hereafter TH99). The basic idea is to use the $T–S$ relationships of the closest T and S profiles in time and space to reconstruct the salinity profile from temperature information only. The approach has proven to be successful in the reconstruction of observed salinity profiles in the western tropical Pacific Ocean when the $T–S$ relationships are taken from observed profiles up to a few weeks before the time of the reconstruction (TH99). In the work presented here, observed $T–S$ relationships are replaced by the $T–S$ relationship of the model background, which is derived locally from the model predicted T and S profiles. The main advantage of this approach compared to employing EOFs is that no learning period is needed. On the other

hand, the scheme relies on realistic model T and S profiles. In order to test the method in a data assimilation framework, experiments have been devised using an ocean global circulation model, in which temperature data are assimilated.

The work is organized as follows: in section 2 the ocean model, the data assimilation system, and the experiments are described. Results from the latter are presented in section 3. A discussion is provided in section 4.

2. Experimental setup

This section presents the experimental setup adopted in this work. The setup chosen is slightly different from that used in the operational mode at ECMWF in that some parameters have been changed. In particular, we use data whose quality control is preprocessed, guaranteeing that the same temperature data are used in all experiments. Furthermore, the maximum depth to which data are assimilated is reduced from 1050 to 425 m, to match the bottom of the Tropical Atmosphere Ocean (TAO) mooring observation profiles. In the following, a brief description of the ocean model is given first. Then the data assimilation system is described and, finally, the two experiments to test the TH99 salinity scheme are outlined.

a. Ocean model

The ocean model used in this work is the Hamburg Ocean Primitive Equation model (HOPE; Wolff et al. 1997), modified by ECMWF for seasonal forecasting in coupled mode (e.g., Stockdale et al. 1998; Alves et al. 1998). Here we only describe its main features. It is a 3D primitive equation model using z coordinates and a variable sea surface height in a global domain. The model's horizontal structure uses an E grid (Arakawa and Lamb 1977) with a horizontal resolution of $2.8° \times 2.8°$ (latitude–longitude) plus an equatorial refinement: the meridional resolution is $0.5°$ within $10°$ of the equator, which changes smoothly from $0.5°$ to $2.8°$ between $10°$ and $30°$. In the vertical there are 20 levels, 12 of which are in the upper 425 m. The parameterization of the vertical mixing uses a Richardson number–dependent K scheme (where K is the vertical eddy diffusivity coefficient), a modification from that of Pacanowski and Philander (1981). The K value is increased mainly within the mixed layer, which is diagnosed as the depth range in which temperatures differ by less than $0.5°C$ from the sea surface temperature (SST). In order to avoid numerical problems with static instability, an ad hoc convection scheme is included, which mixes two adjacent model levels if $d\rho_\theta/dz > 0$ locally, where ρ_θ is the potential density.

The model is forced by daily average momentum, heat, and fresh water fluxes taken from the ECMWF atmospheric analysis system. In order to avoid unrealistic drifts, additional weak restoring terms (timescale
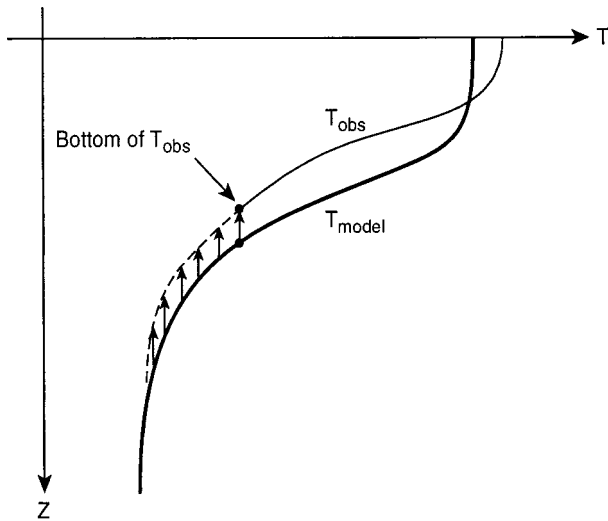
FIG. 1. Schematic of the vertical displacement (first part of the TH99 scheme). The displacement is the difference between the depth of the deepest observed (or, as in our case, the output of the OI) temperature (thin solid line) and the depth of the same temperature in the model profile (bold solid line). This displacement is then used to lift (as in the figure) or lower the model profile in order to complete the observed profile below the deepest observed T (dashed line).

FIG. 2. Schematic of the data assimilation system. TH99 scheme is the salinity scheme.

of 1 yr) are applied to the three-dimensional T and S fields by using annual climatological values from Levitus and Boyer (1994) and Levitus et al. (1994, hereafter referred to as Levitus). An additional weak relaxation (timescale of 1 yr) is applied to the Levitus surface S implying a damping time of 6 months for the surface salinity. A strong relaxation (timescale of 3 days) is applied to the surface temperature using weekly analyses (Reynolds and Smith 1995) provided by the National Centers for Environmental Prediction (NCEP).

b. Data assimilation system

The data assimilation method used in this study is an optimal interpolation (OI) derived from Smith et al. (1991). The observations are subsurface temperature measurements, obtained mainly from the U.S. National Oceanographic Data Center through the Global Temperature Salinity Pilot Project (GTSPP) data distribution network. The main components of the observing system are the XBTs and TAO moorings in the equatorial Pacific. TAO-type moorings in the tropical Atlantic from the developing Pirata array and Profiling Autonomous Lagrangian Circulation Explorer (PALACE) float data distributed through the Global Telecommunication System (GTS) are also used, even though these data types are much more recent and only have an impact towards the end of the experiments. The OI method is used to map these subsurface temperature observations onto the model background. The observed T profiles are first interpolated onto the model levels, which are treated independently from each other in the OI. The OI of the
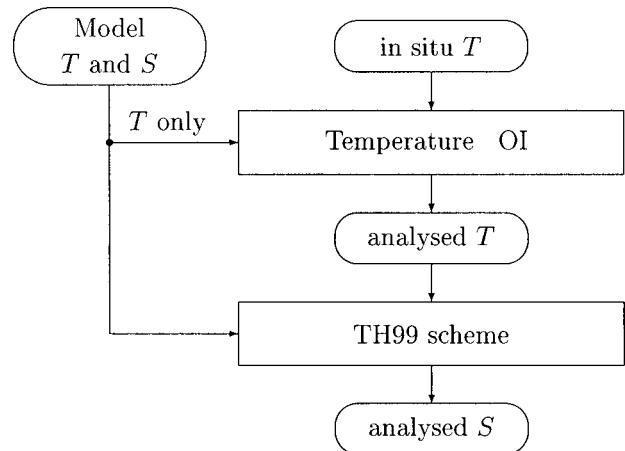
temperature field (with the model T used as a background) is performed every 10 days, using observations grouped in 10-day bins. Following Smith et al. (1991), the background is given the same weight as an individual observation. The background errors are expressed as anisotropic and inhomogeneous Gaussian functions whose correlation length scales near the equator are 1500 km zonally and 200 km meridionally. In all the experiments described in this paper the assimilation is done over the levels from 2 to 12 (i.e., between 30- and 425-m depth). For further detail on the OI implementation in the HOPE model see Alves et al. (1999).

In order to obtain the updated vertical salinity profiles (i.e., the salinity analyses), the temperature profiles obtained by the OI are processed through the TH99 scheme. This procedure is performed on each model grid point. This scheme is in two parts. First, a vertical displacement of the model background profile to match the bottom of the analysed T profile is made. The displacement corresponds to the difference between the depth of the deepest analysed temperature and the depth of the same temperature in the model profile (an example is shown in Fig. 1). The salinity profile is also shifted by the same amount. This first part of the scheme assumes that isopycnal surfaces are often displaced even below the depth to which observations usually extend, for example, by internal waves. The matching should also help to prevent convective adjustments at the bottom of the observed profile. However, if the temperature at the bottom of the analysed profile is outside the T range of the model background, no displacement is performed. Typically, this may happen in coastal regions and at high latitudes. Second, the scheme computes an S analysis within the depth range of the T profile, using the T–S relationships from the model T and S background profiles, at each grid point. For example, at a T observation of 20°C, the analysed S will be the same as the S present at the depth of 20°C water in the model

TABLE 1. The three experiments.

Expt	Period (yr)	Assimilation
CNT	1993–98	None
TOI	1993–98	OI
TOIS	1993–98	OI + TH99

profile. For profiles with T inversions, the nearest (in z) T match is used.

No information other than the temperature analysis (OI in the present case) and the model T and S profiles is needed for the TH99 scheme to work (see Fig. 2). It is known, however, that T–S preservation is not a good hypothesis when nonisentropic processes are dominating (e.g., in the mixed layer or in the vicinity of river inflow) for which T and S variations may be highly uncorrelated. Therefore, if the OI temperature is outside the range of the model T profile (as typically happens near the surface), then the model salinity is not modified. Also, in order to avoid extrapolating T–S relationships of near-surface water to deeper layers, the model T–S relationship from the upper 50 m of the water column

is used only if the corresponding OI temperature is also near the surface. Otherwise, no change is made to the model salinity.

In addition, a latitudinal filter has been applied to the salinity and temperature increments such that the whole salinity increment is applied only within 30° of the equator. Outside this region, the weight given to the salinity analysis diminishes linearly to zero at latitudes poleward of 60°. This is done to avoid implementing the TH99 scheme in areas where the stratification is weak and $S(z)$ persistence is more appropriate (see Emery and Dewar 1982).

c. Description of the experiments

Three experiments, listed in Table 1, are run to test the TH99 salinity scheme. They all use the ocean model setup described in section 2a. The initial conditions are taken from a spinup run which has been relaxed with a 10-day timescale to the Levitus climatology at all depths. The experiments are run for the period 1993–98.

To assess the impact of the TH99 salinity scheme on the OI analysis, two experiments are considered: one in
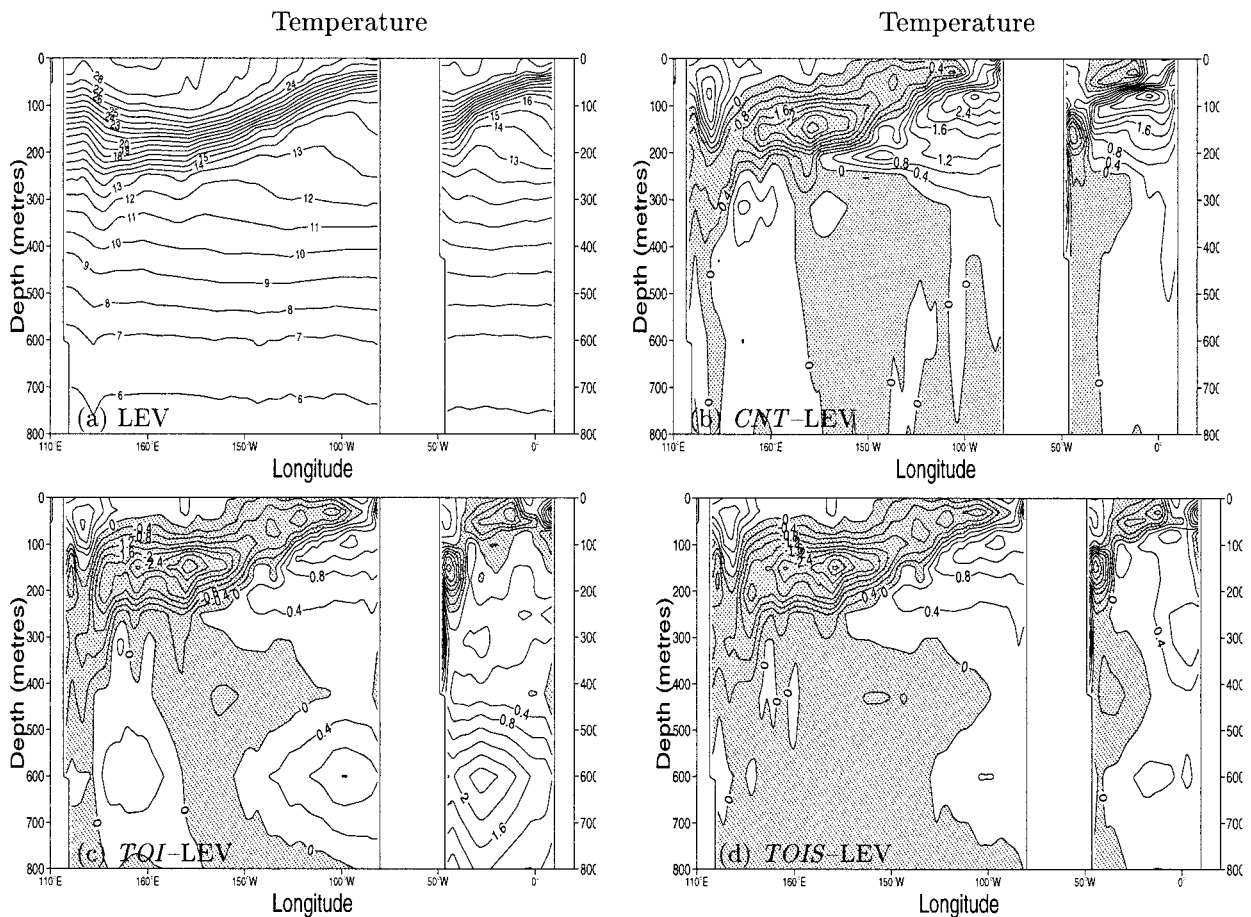

FIG. 3. Equatorial sections of temperature. (a) Annual mean Levitus climatology, (b) the difference between expt. CNT and Levitus averaged over the 6-yr mean (1993–98), (c) same as in (b) but for expt. TOI, and (d) same as in (b) but for expt. TOIS. Negative values are shaded. Contour interval is 0.4°C.

which the TH99 salinity scheme is added to the OI (TOIS) and the other in which only the OI is used (TOI). In both experiments the temperature observations are presented to the OI procedure first. In TOIS the TH99 scheme is applied locally as a second step at each model grid point, as described in section 2b. The T and S increments thus calculated are then uniformly added to the model background over a 10-day period, in order to allow the model to gradually adjust to the analyzed density field. For reference, a run with no data assimilation is also performed (CNT), which will be used to check how the data assimilation affects systematic model errors.

3. Assimilation results

In this section we analyze the impact of the TH99 salinity scheme, by comparing the two runs TOIS and TOI with observations (e.g., Levitus climatology) and the experiment CNT. We first analyze a 6-yr mean in section 3a and then we investigate the salinity and the sea level variability in sections 3b and 3c, respectively.

a. Analysis of mean fields

To investigate whether TH99 can improve the mean state, we examine time-averaged fields from the entire run (i.e., the 6-yr mean 1993–98). We first consider the equatorial section through the Pacific and Atlantic Oceans. The equatorial Pacific is an area relatively rich in T data and it is also very important for seasonal forecasting.

Figure 3 shows temperature sections along the equator for the Pacific and Atlantic Oceans. In the figure, panel (a) shows the climatological average from Levitus, and panels (b)–(d) show the differences between CNT, TOI, TOIS means and Levitus. Although we use Levitus as a measure of climatology, it should be born in mind that it is not an absolute measure of the mean state of the oceans. It is known, for example, that the TAO thermal data are rather cooler than Levitus in the western Pacific, either because of a different averaging period (Levitus used all data from 1900–93) or a better data coverage than Levitus, during the TAO period. We compared the Levitus climatology with the TAO climatology from Yu and McPhaden (1999), and found that TAO was colder by more than 2°C around 150-m depth in the western Pacific (Fig. 4).

The dominant feature in Fig. 3a is the sloping thermocline, which is an important feature of these two oceans. The CNT experiment shows substantial deviations of up to 3°C at the depth of the thermocline. The CNT experiment is warmer than Levitus in the eastern Pacific and in the Atlantic Ocean, and colder in the western Pacific. The cooler mean temperatures in the western Pacific are in fact in good agreement with the TAO data but not with the Levitus data, as will be seen later. However, the warmer temperatures in the Atlantic and eastern Pacific Oceans are due to systematic bias
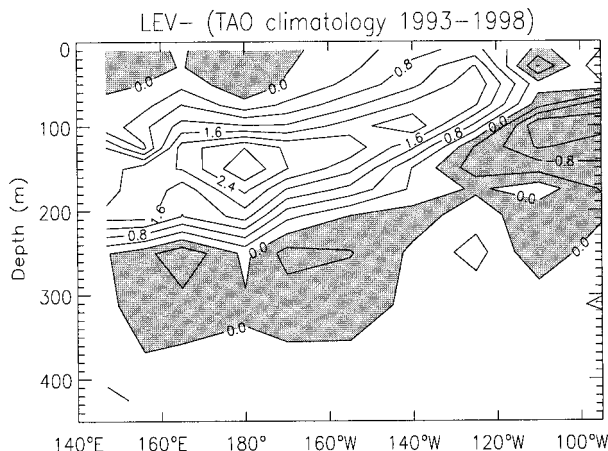

FIG. 4. Equatorial section of temperature. Difference between the annual mean Levitus climatology and the 1993–98 TAO climatology. Negative values are shaded. Contour interval is 0.4°C.

in the CNT experiment. This bias is linked to a too diffuse thermocline in the model, possibly due to limitations of the mixing scheme combined with a poor vertical resolution.

Figures 3c and 3d show that in TOI and TOIS, some of these temperature differences are substantially reduced as a result of temperature assimilation. The warm biases at the thermocline level in the eastern Pacific and across the Atlantic are very substantially reduced in both assimilation experiments. The temperature differences in the western Pacific remain substantially unchanged, however, consistent with the TAO data being colder than Levitus in this region, as shown in Fig. 4. Since the long-term mean of CNT is already consistent with the TAO data, the assimilation of temperature data does not change the mean thermal structure of CNT in the subsurface western Pacific very much.

Below the thermocline, however, significant differences with respect to Levitus, appear in TOI, which is up to 1.2°C warmer than Levitus around 600 m in the eastern Pacific, and more than 2°C warmer than Levitus at 600 m in the Atlantic Ocean. It can be noted that this would correspond to a vertical displacement of the isotherms on the order of 100 to 200 m at these depths. The differences between TOI and Levitus are thus quite large. These spurious differences are not present in CNT and must, therefore, be induced by the assimilation. They disappear in TOIS showing that the TH99 scheme helps to improve the deep ocean thermal structure in the assimilation. A discussion of the causes of the differences in the two experiments TOI and TOIS is deferred to later in this section, after introducing the salinity fields.

Figure 5 shows the salinity sections corresponding to the temperature sections from Fig. 3. The Levitus climatology (Fig. 5a) is characterized by relatively fresh water close to the surface, an intermediate salinity maximum around the depth of the thermocline, and mono-

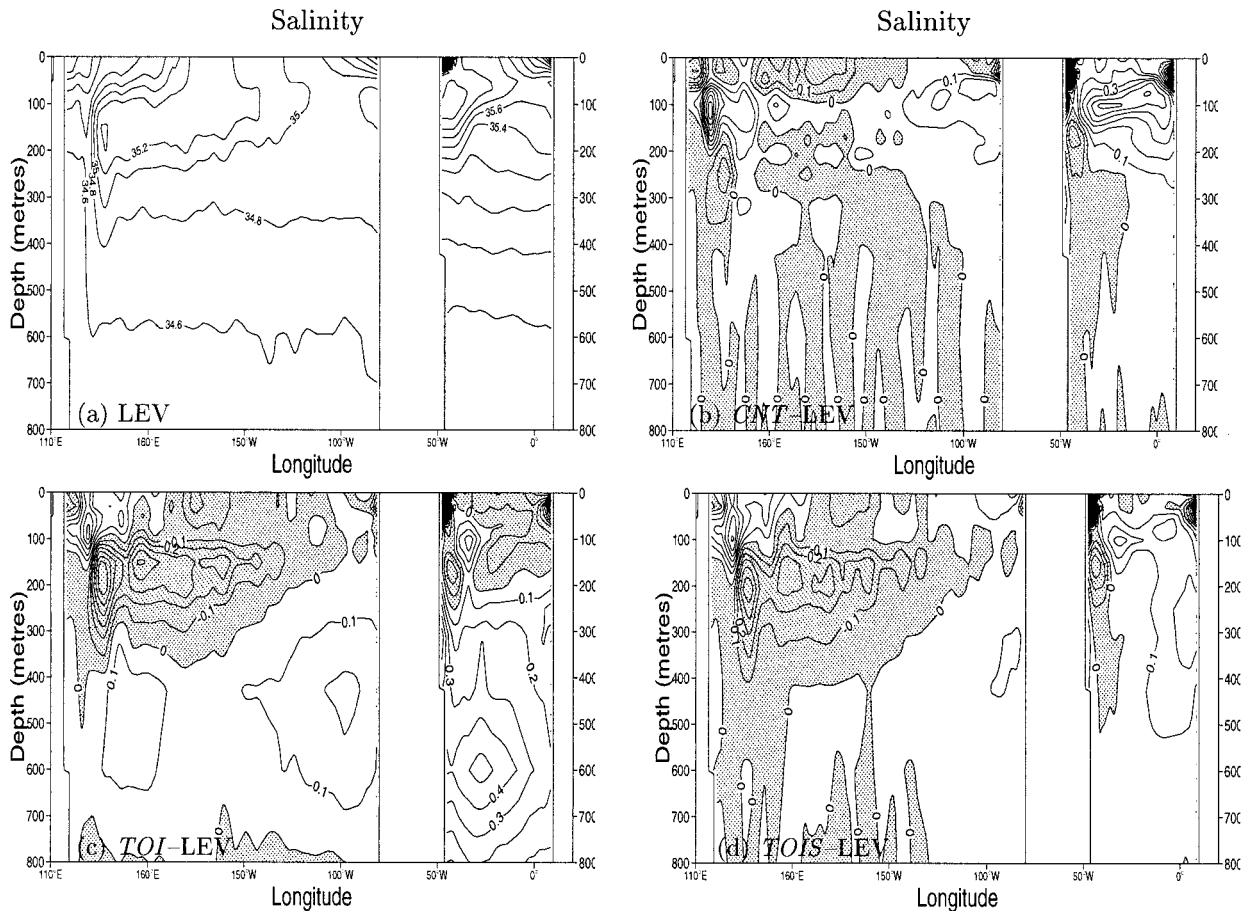Salinity   Salinity

FIG. 5. As in Fig. 3 but for salinity. Contour interval is 0.1 psu.

tonically decreasing salinity below about 200 m. Low surface salinities are present at both the eastern and western boundaries in both oceans due to strong precipitation and/or river runoff. The subsurface salinity maximum is most pronounced in the western part of the basins. Because of errors in the specified surface freshwater flux and in the model formulation, CNT is different from Levitus (Fig. 5b). It is slightly fresher near the boundaries in the surface layer, and saltier around the subsurface salinity maximum. However, for the section shown, the departure from climatology is small below 200 m.

Figure 5c shows that the assimilation of temperature data in experiment TOI introduces large changes in the salinity field in the subsurface. In particular, salinity is lower than Levitus at around 200 m (by up to 0.6 psu in both the western Pacific and Atlantic). Below 300 m, salinity is higher than Levitus (by up to 0.2 psu in the Pacific and 0.5 psu in the western Atlantic). This indicates a transfer of salt from intermediate to deeper layers, as will be discussed later. The additional correction of salinity in experiment TOIS (Fig. 5d) results in smaller differences with respect to Levitus salinity, and in particular the differences in TOI below 300 m

in experiment TOIS essentially disappear. At the thermocline level, differences are also notably diminished in the western Pacific ocean compared to TOI. All in all, below the depth of 50 m, TOIS shows a promising improvement over TOI, when compared to Levitus. The behavior of all three experiments is very consistent in the surface layer, but as mentioned earlier, we do not expect the TH99 scheme to improve surface-layer salinity.

We can now start discussing possible causes of the differences between TOI and TOIS. Figure 6 shows meridional sections along 30°W of climatological temperature and of an instantaneous model output from TOI. After only 3 months, the temperature structure reveals large errors in the equatorial region. The isotherms between 5°N and 5°S have been displaced downward in an unrealistic way in TOI. This is most likely caused by strong vertical mixing or convection. Very weakly stratified or unstable water columns can be created as the result of temperature assimilation in regions where there is a subsurface salinity maximum. Below this maximum, S decreases with depth and static stability is sensitively dependent on the temperature stratification. If the temperature increments given by the OI scheme in
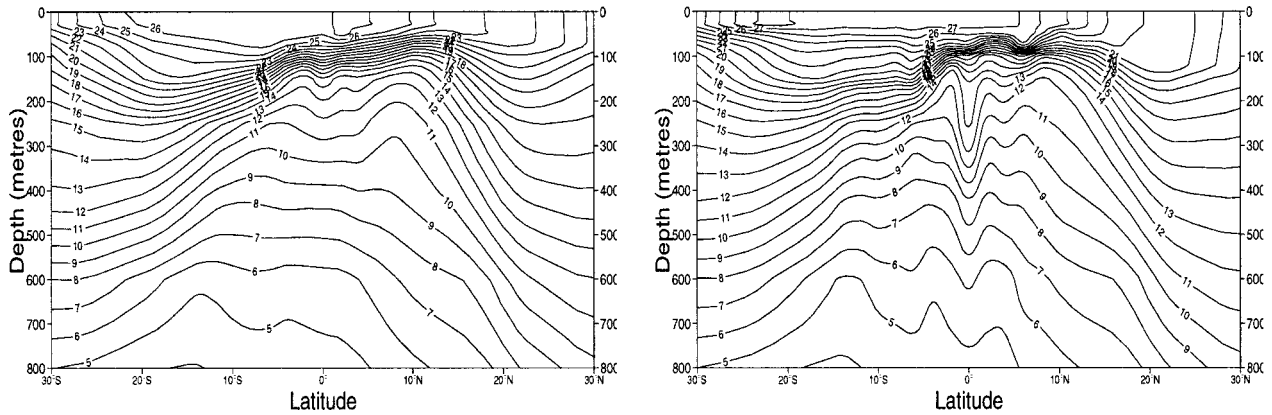
FIG. 6. Meridional temperature section at 30°W. (left) Initial conditions (i.e., climatology). (right) Instantaneous field after a 3-month model integration with an OI temperature assimilation (expt TOI).

TOI are such as to decrease the vertical T stratification in these regions, (while S is left unchanged), the water column may become statically unstable. The model mixing scheme then responds by spuriously increasing the vertical mixing. This is strongly reduced by the TH99 scheme in TOIS: the scheme adjusts the salinity profile in order to preserve T–S characteristics and thus ensures static stability.

The spuriously increased mixing is most likely to occur where the salinity maximum in the main thermocline is relatively prominent or, more generally, when the salinity gradient below the S maximum is large. This explains why differences between TOI and TOIS are more pronounced in the equatorial Atlantic where the subsurface S maximum is stronger than in the Pacific.

An objective way of identifying those areas most likely to be affected by the enhanced mixing is provided by the following analysis. The stability of the water column can be expressed as the derivative of $\rho_\theta = \rho_\theta(\Theta, S)$ with respect to depth (z positive upward):

$$\frac{d\rho_\theta}{dz}(\Theta, S) = \left(\frac{\partial \rho_\theta}{\partial \Theta}\right)_S \frac{d\Theta}{dz} + \left(\frac{\partial \rho_\theta}{\partial S}\right)_\Theta \frac{dS}{dz}$$

$$= -\alpha\rho_\theta \frac{d\Theta}{dz} + \beta\rho_\theta \frac{dS}{dz}, \quad (1)$$

where ρ_θ is the potential density, Θ the potential temperature, and α and β are the thermal and haline expansion coefficients. In a statically stable water column $d\rho_\theta/dz$ is negative. In TOI the temperature profile is changed while the S profile is retained. If dS/dz is positive, this can lead to a statically unstable profile if temperatures are reduced at that depth by the OI. The critical value of the temperature stratification $(d\Theta/dz)_U$, which would cause convection to begin (when $d\rho_\theta/dz$ is zero), is given by:

$$\left(\frac{d\Theta}{dz}\right)_U = \frac{\beta}{\alpha}\frac{dS}{dz} = \gamma\frac{dS}{dz}, \quad (2)$$

where $\gamma = \gamma(\Theta, S) > 0$.

If we assume, as shown by TH99, that temperature variability in the thermocline occurs mostly through vertical displacements of the water masses, it is possible to compute the minimum vertical displacement of the T profile for which this will happen. The smaller this value, the greater the risk of spurious convection. Figure 7 shows the results of such evaluation with the temperature and salinity fields taken from the Levitus climatology along the equatorial section (left) and the 30°W meridional section (right). The solid lines show the minimum displacement, while the dashed lines give the depth at which instability occurs. The plot on the left shows that the Atlantic sector (between 50°W and 10°E) is more prone to instability than the Pacific sector. In the Atlantic, upward shifts of the temperature profile of between 15 and 60 m (solid line) are generally sufficient to make the water column unstable at depths that vary between 90 and 240 m (dashed line). In the Pacific these displacements are always more than 70 m and generally well over 100 m.

This analysis yields a more rigorous confirmation of what could have been deduced from the climatological S in Fig. 5a: the S maximum in the Atlantic is up to 1 psu larger than in the Pacific, but the S values at depth are very close in the two oceans.

The smaller amount of temperature data collected in the Atlantic is another contributing factor as to why TOI and TOIS differences are more pronounced in the equatorial Atlantic than in the Pacific, in particular in the thermocline. In the Atlantic during 1993–98 the main source of T profiles are XBT casts along shiptracks, so that observations at one location are only made a few times per year. Some of these will tend to generate spurious mixing in TOI and to erode both the temperature and salinity stratification. The only compensation will be the relaxation to climatology, which acts on the slow timescale of 1 yr. On the other hand, in the Pacific Ocean there are frequently repeated observations at the same location from the TAO array. Once the salinity gradients have been eroded (this can be seen happening in Fig.
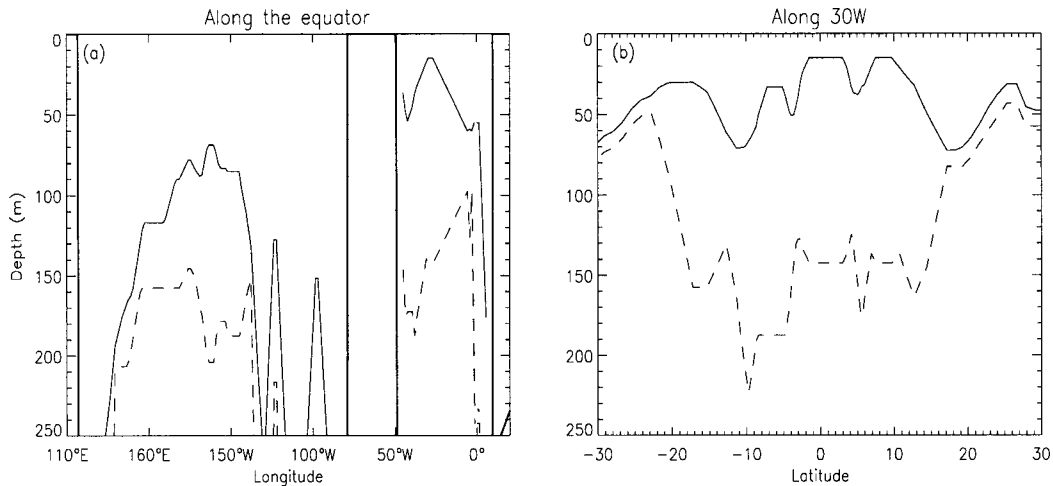
FIG. 7. Minimum vertical displacement that would destabilize the water column (solid line) and depth of the corresponding level (dashed line) along the (a) equatorial section and (b) Atlantic meridional section at 30°W.

8), the subsequent temperature observations can constrain the temperature field without generating more spurious mixing or convection. The temperature field is thus very well constrained whereas the salinity field is still in error.

Note that in TOI, the assimilation makes no temperature increments below 425-m depth. This is an extreme "data sparsity" problem and means that if the analysis starts to go wrong, there is nothing to bring it back other than the very slow relaxation to climatology. Thus, once a warm column begins to develop at these depths, it may be hard to stop. Extending the temperature analysis to lower depths might reduce this problem, or at least push it down deeper. In the experiments presented here, we chose 425 m instead of the operationally used 1050 m in order to match the depth to which TAO observations extend. It is mainly XBT observations that extend to greater depth.

To further study the impact of the TH99 scheme, we consider now a 6-yr mean meridional section at the same location as for Fig. 6 (30°W). Figures 8a–d show the T and S fields for both TOI and TOIS and the difference between the two experiments (Figs. 8e,f). The T field is characterized by a tight thermocline between 8°S and 13°N. The S field has two surface maxima at around 17°S and 24°N, from both of which subsurface salinity maxima extend toward the equator. In Figs. 8a and 8b, starting at the base of the main thermocline, an anomalous warm and salty water column is seen in TOI in the neighborhood of the equator. Such a feature is not present in the Levitus climatology: it is a manifestation of the spurious mixing activity discussed previously. On the other hand, the T and S fields of TOIS look more realistic (Figs. 8c,d), with only a slight downward bulge in the salinity field at the equator and a corresponding, though smaller bulge in the T field (5° and 6°C isotherms). This suggests that some mixing may still be occurring intermittently

in the TOIS experiment, probably due to the fact that the assimilation does not take into account the actual depth of each observation profile (the deepest assimilation level is fixed, at 425 m). The difference between TOI and TOIS along this section (Figs. 8e,f) shows large discrepancies in T and S, especially in the 7°S–8°N band, where the stability analysis (Fig. 7b) shows that instabilities are most likely.

We now investigate the effect of the differences in T and S on the density field. Figure 9a shows an equatorial section of density and Figs. 9b,c of temperature and salinity, respectively. In both oceans TOI is lighter than TOIS at the pycnocline level (around 150 m) and denser below. This is exactly what we would expect if TOI has had enhanced convection, that is, denser water convecting down from above. In the Pacific Ocean, T differences between the two experiments are small (Fig. 9b). The density differences are thus mainly linked to the salinity (e.g., saltier water in TOI below the pycnocline results in denser water). In the Atlantic Ocean, there is a competing effect of T and S on the density field (e.g., with TOI warmer and saltier below the thermocline). However, the salinity effect is once again dominating.

It is interesting to consider these density differences because they have an impact on sea level. Because of the compensating effects of T and S differences, and because of vertical compensation between denser water in TOI below the pycnocline and lighter water above, the overall difference in sea level is generally small. Along the equator in the Pacific and in the Atlantic, TOIS has a higher sea level than TOI, but the difference does not exceed 2 cm for the 6-yr average (not shown).

b. Salinity variability

In the previous section we have shown that the use of the TH99 scheme generally improves the mean state

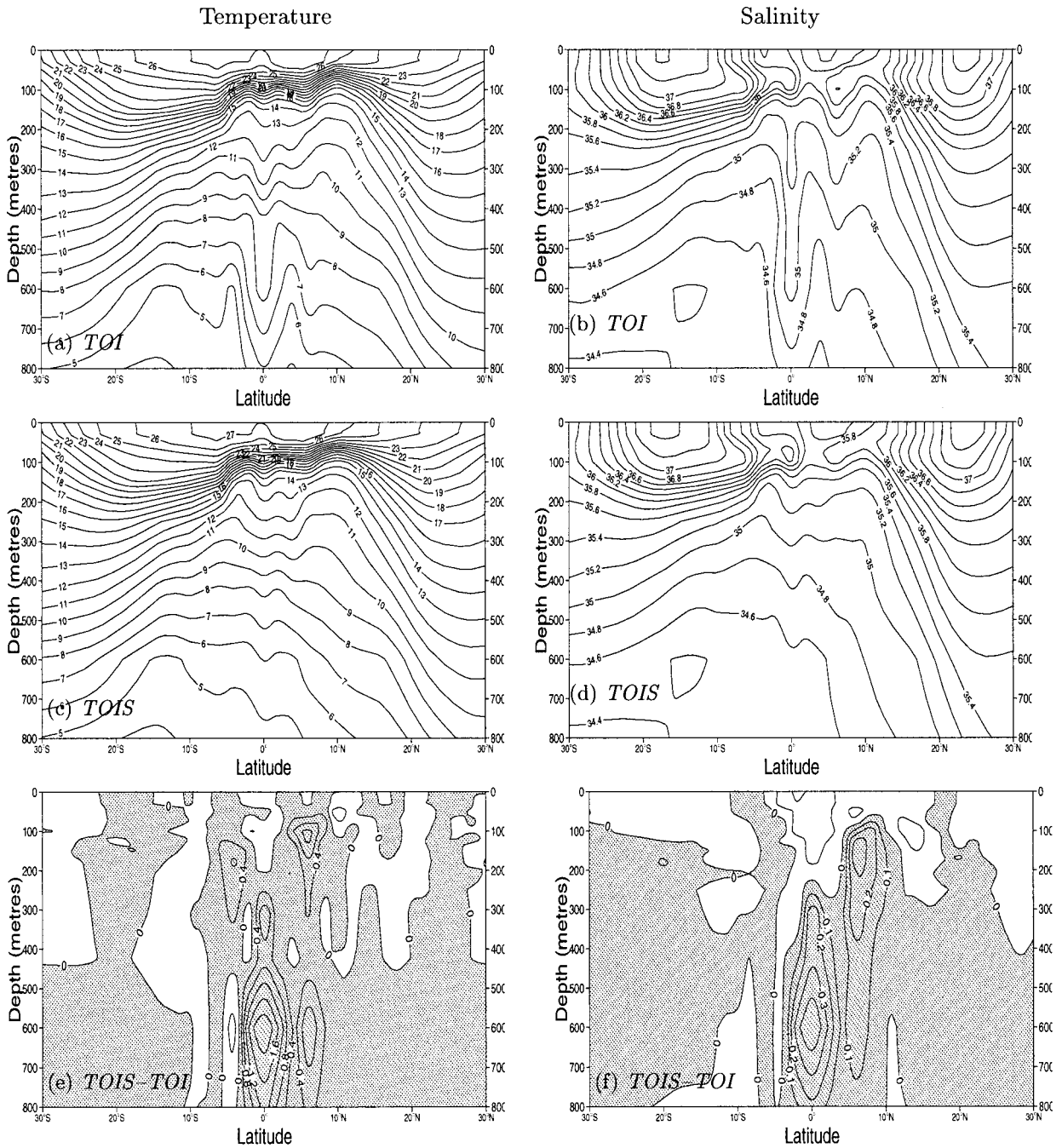Temperature   Salinity

FIG. 8. Meridional sections at 30°W of the 6-yr mean (1993–98). (a) Temperature and (b) salinity for the OI-only run (expt TOI), (c) temperature and (d) salinity for the OI plus salinity scheme run (expt TOIS), (e) TOIS − TOI temperature difference, and (f) TOIS − TOI salinity difference. Negative values are shaded. The enhanced vertical mixing is evident in TOI between 7°S and 8°N (a), (b). This causes large differences both in T and S between TOIS and TOI (e), (f).

of the ocean. However, for seasonal climate forecast initialization, the variability is also of concern. In this section we examine the salinity variability both by looking at differences between the time-varying salinity fields in TOI and TOIS and by comparing them with other modeling and observational results.

To begin with, we look at integrated measures of the salinity in two regions, the Niño-4 region in the western Pacific (5°N–5°S, 160°E–150°W), and a box spanning the Equatorial Atlantic from 5°N to 5°S. Figures 10a,b show the average salinity in the top 280 m of the water column and the average from 60–280 m, respectively, for the Niño-4 region. Figures 10c,d show the same quantities for the Atlantic box.
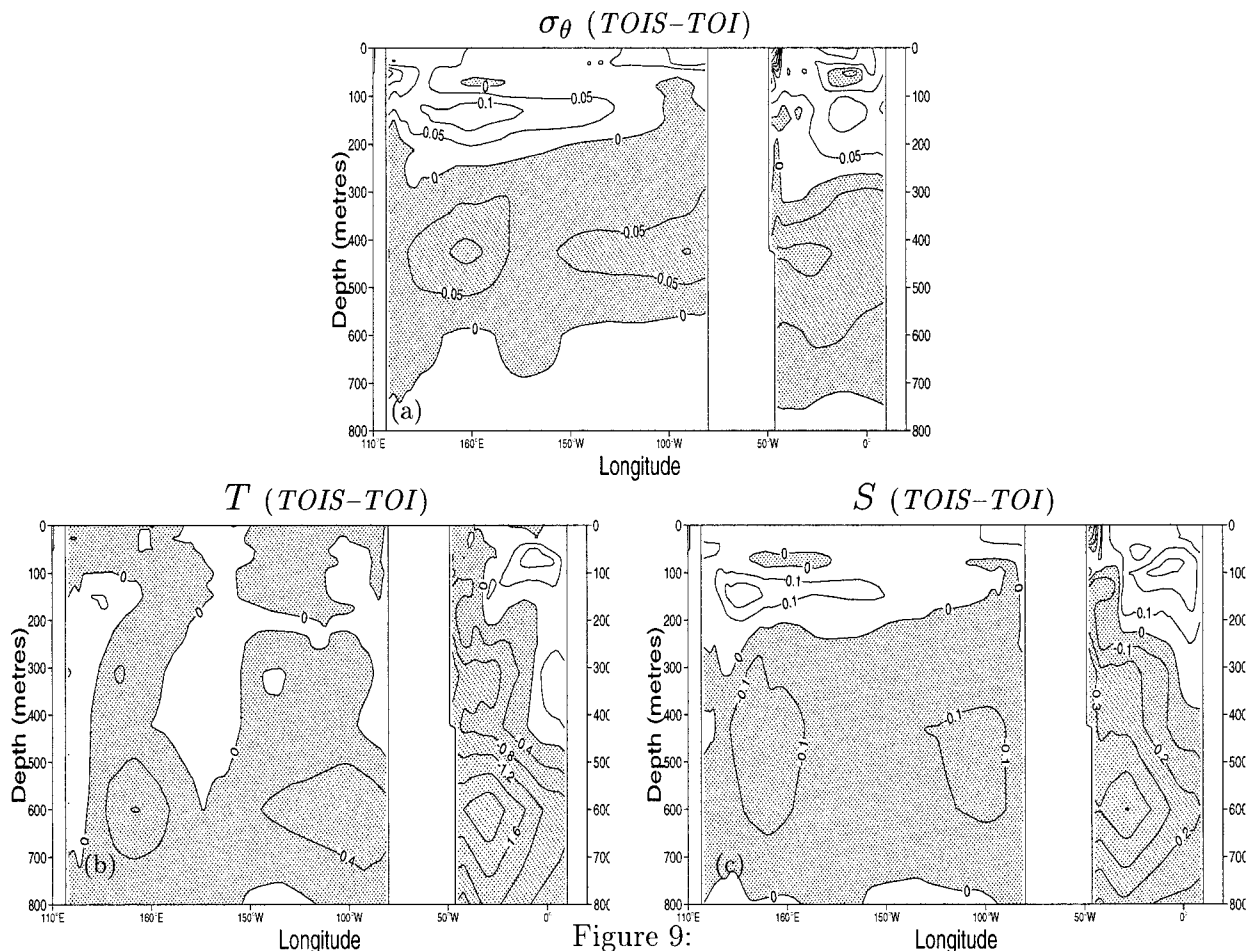
σ_θ $(TOIS-TOI)$

T $(TOIS-TOI)$

S $(TOIS-TOI)$

Figure 9:

FIG. 9. Equatorial section of the difference TOIS − TOI for the 6-yr mean (1993–98) for (a) σ_θ, (b) temperature, and (c) salinity. Negative values are shaded.

It is immediately clear that the integrated salinity in the TOI run drifts downward rapidly as soon as assimilation is applied and that most of this drift takes place below the mixed layer, that is, below 60 m. In contrast the TOIS run maintains its mean salinity values as assimilation begins. This leads to average salinity differences of up to 0.05 psu in the Niño-4 region and up to 0.2 psu in the equatorial Atlantic in Figs. 10b,d. The reason for the lower salinity in TOI is the loss of salt to layers below 280 m due to spurious convection. The salinity variability is large in the surface layers and is fairly similar in each run since the surface forcing is virtually the same in the two runs. The seasonal cycle is particularly clear in the Atlantic box, while interannual variations are clear in the Pacific where the 1997 ENSO shows up very strongly in Fig. 10a. The freshening in 1997 appears to be confined to the near-surface layers since Fig. 10b shows a much smaller signal.

Variability in the 60–280-m layer shows more interesting signals. In the Niño-4 region the salinity variability still shows a seasonal cycle, but whereas in TOI this has a fairly constant amplitude, in TOIS the am-

plitude appears to increase for four years culminating in the 1997 ENSO event, after which the salinity cycle returns to much lower values. If this is a real signal it would invite speculation on the role of salt in the warm water pool in the runup to ENSO events. Clearly salinity variability is larger in the TOIS run but it is difficult to know whether this is realistic. In the Atlantic box the salinity variations show little annual cycle and are less correlated between the TOI and TOIS runs.

Observational salinity data with information about temporal variability are very sparse. We found no suitable comparison data at all in the Atlantic. The section along 165°E in the western Pacific is one of the best observed but even here data coverage is poor. The most thorough analysis of this section is published in Kessler (1999, hereafter K99). Figure 2 of K99 shows the evolution of salinity as a function of depth and time for the region 3°–5°S. From the beginning of 1993 the figure shows that subsurface salinity increases until the beginning of the ENSO of 1997. Figure 4 of K99 shows a similar temporal trend and suggests that a wider range of latitudes is involved. This is at least consistent with
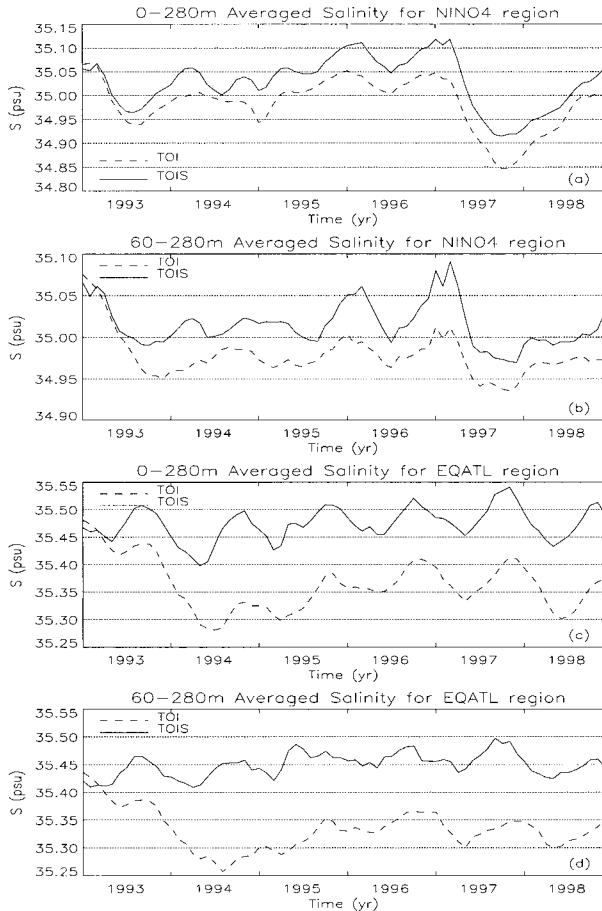
FIG. 10. Temporal evolution of the salinity averaged over (a), (c) 0–280 m and (b), (d) 60–280 m for the (a), (b) Niño-4 region and (c), (d) the equatorial Atlantic for TOI (dashed) and TOIS (solid).

FIG. 11. Salinity as a function of depth and time at (3°–5°S, 165°E) for (a) TOIS and for (b) TOI. Contour interval is 0.2 psu. The times when observations are available are shown by the vertical lines.

the increasing salt trend over the whole Niño-4 area shown in Figs. 10a,b from mid-1993.

Figure 11 shows the model equivalent of K99 Fig. 2, that is, the salinity average 3°–5°S at 165°E for the assimilation runs. Vertical lines show the times when this area was observed, indicating the data used to construct K99 Fig. 2. The annual sampling is clearly inadequate to capture all the changes taking place in the salinity layer. Again there is a clear suggestion from the TOIS plot (Fig. 11a) that salinity is increasing from early 1993 to mid-1996, as presented in K99. Notice also the sudden deepening of the salinity maximum and the downward spread of salt in TOI in the second half of 1997. This is an example of the intermittent nature of the spurious convection generated if salinity is not accounted for during the assimilation of T profiles.

Finally we look at two specific CTD profiles from this same area. Ji et al. (2000) looked at two CTD profiles at 2°S, 165°E, one from 2 May 1995 (hereafter CTD95), and the other from 10 July 1996 (hereafter CTD96). They did this to try to explain an observed discrepancy in sea level between these dates, which
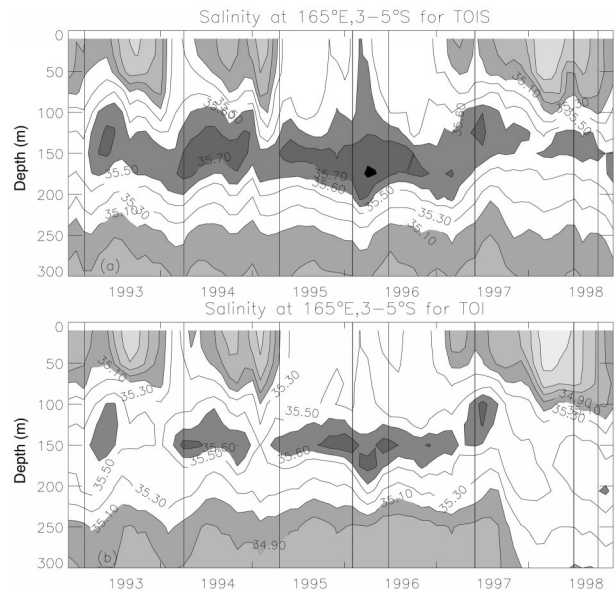
could not be explained by the T profile differences. They found that the CTD95 salinity profile was fresher than the CTD96, down to a depth of about 180 m. Ji et al. (2000) argue that the interannual S variation would explain the 5–10 dyn cm sea level difference.

Figures 12a and 12b show the same two CTD profiles compared with the May 1995 and July 1996 monthly average salinity profiles for TOI and TOIS. Note that on a timescale of one month, the CTD rms variability could be as large as 0.2 psu in the thermocline and even larger closer to the surface (Fig. 2 in TH99). As a reference, the Levitus annual salinity profile at (2°S, 165°E), to which TOI and TOIS are weakly relaxed, is also plotted in Figs. 12a,b.

The agreement of the S profiles for May 1995 for TOI and TOIS with CTD95 are reasonably good from 100–200 m through the salinity maximum (Fig. 12a). However, at deeper levels TOIS is clearly more realistic, being much closer to the observations and to Levitus. The CTD96 observations clearly show higher salinities than CTD95, and both TOI and TOIS also show an increase to some extent. The salinity maximum in TOIS is, however, closer in value and in depth to the observed and again at deeper levels TOIS is also closer to the observed profile. Vossepoel and Behringer (2000) also compared their own assimilation results for salinity with a similar set of CTD casts. Their near-surface fit to CTD96, in Fig. 16 of Vossepoel and Behringer (2000), is 0.25 psu compared to 0.08 psu in TOIS, and at the depth of the S maximum it is 0.75 psu compared to 0.4 psu in TOIS.
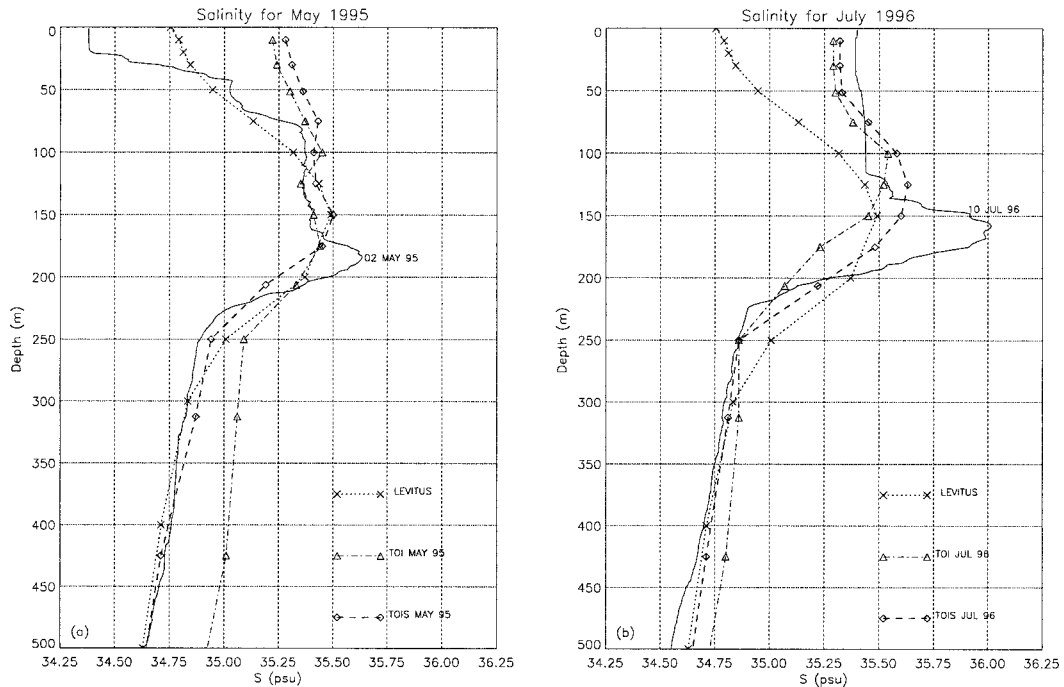
Fig. 12. Salinity profiles at (2°S, 165°E) from instantaneous CTD data (solid lines) and monthly averages for TOI (dash–dotted) and TOIS (dashed) for (a) May 1995 and (b) Jul 1996. Also plotted is the annual Levitus salinity profile (dotted) to which TOI and TOIS are relaxed.

c. Sea level variability

We will now examine impact of assimilation on the sea level variability. Figure 13 shows the variations in the average sea level in the Niño-4 region for the two model runs, and for the TOPEX/Poseidon (T/P) altimeter data. Most of the variability is due to the seasonal cycle but there are significant interannual variations which are also clear, and the ENSO of 1997/98 stands out strongly. It is clear that both model runs do a good job at tracking the sea level changes through this period, including the interannual component, and it is not really possible to distinguish the runs on the basis of sea level comparisons. This is not unexpected because the erroneous vertical redistribution of salt produced in the TOI assimilation run should not affect the mean density of the water column since it occurs from convection, and therefore the dynamic height component of sea level is
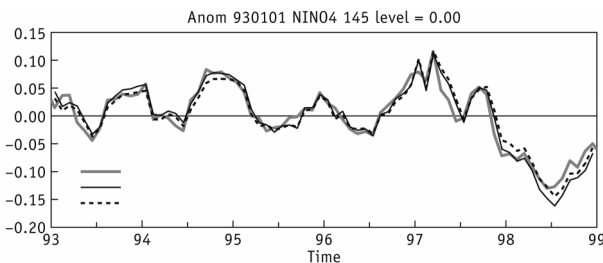
unlikely to change. We note that neither run shows any serious problems in 1996 where Ji et al. (2000) identified a sea level discrepancy in their model due to salinity errors. Differences between TOI and TOIS, as well as between each of them and the altimeter data, are generally less than 3 cm for this region (after removing the 1993–95 mean in each case).

In Figs. 14a,b we show a comparison between the T/P sea level observations and TOIS in terms of (a) rms errors and (b) correlations for the period 1993–98. These plots have been constructed by taking the T/P gridded products (Le Traon et al. 1998) and the corresponding model fields. Note that the seasonal cycle has already been removed from these figures so that they represent a comparison of interannual variability. Along the equator in the Pacific, the agreement between the assimilation experiment and T/P is good with rms errors with respect to T/P at about 3 cm. The correlation between T/P and model sea level (Fig. 14b) is larger than 90% in the equatorial Pacific. In the equatorial Atlantic the interannual signal is small and the correlation exceeds 80% only in a limited domain. Similar figures for the TOI experiment show essentially the same level of agreement with the T/P data.

The better performance of the Pacific over the Atlantic is partly due, as noted in section 2b, to the larger amount of temperature data available for assimilation in the Pacific. In the Atlantic, T observations are more sporadic since they derive from the XBT network rather than the TAO-type array in the Pacific that reports daily.

Fig. 13. Sea surface height for TOI, TOIS, and the TOPEX/ Poseidon for the Niño-4 region as a function of time.
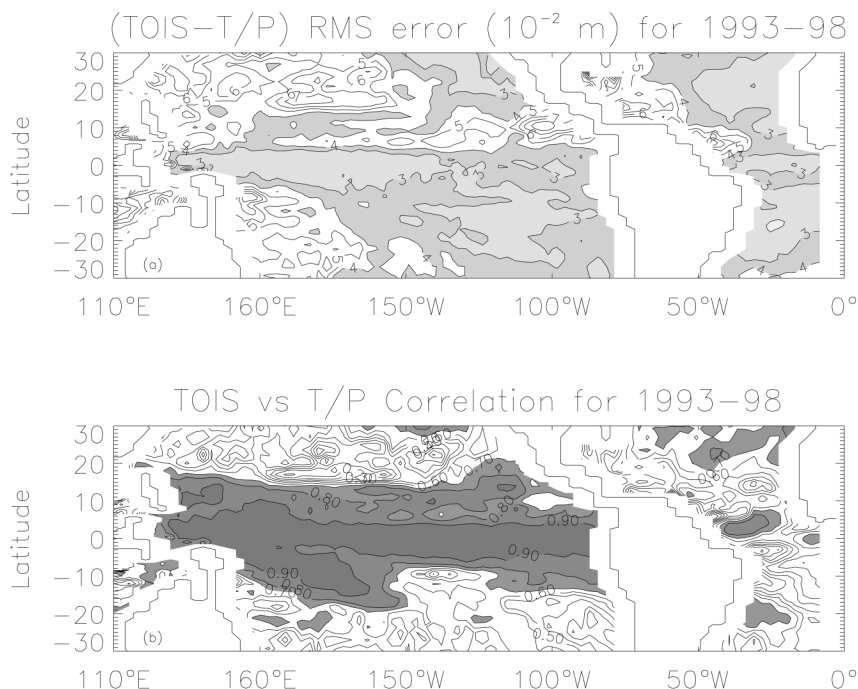
FIG. 14. (a) Sea surface height rms errors and (b) correlations for TOIS with respect to TOPEX/ Poseidon for the period 1993–98. Contour interval in (a) is 1 cm and shading for values smaller than 4 cm. Contour interval in (b) is 0.1 (10%) and shading for values greater than 0.7 (70%). Data are masked in the vicinity of land points.

4. Discussion

The salinity scheme proposed by Troccoli and Haines (1999) has been applied to the ocean model used at ECMWF, by combining it with the preexisting temperature optimal interpolation (OI) procedure. An experiment in which salinity was corrected (TOIS) has been run for the 1993–98 period and compared with one in which only temperature is updated (TOI). The 6-yr mean analysis has shown promising results for TOIS, with significant salinity improvements, with respect to TOI, especially below 50-m depth. Indeed, where TOI leaves $S(z)$ unchanged in regions where salinity decreases with depth, this can lead to first-order errors in the model mean state. The water column can become statically unstable leading to spurious vertical mixing when the temperature increment tends to decrease the thermal stratification. This has a particularly dramatic effect in the tropical Atlantic where there is a strong salinity maximum and where there are sparse measurements to constrain the temperature field. In the experiment TOIS, these first-order errors are virtually eliminated as the TH99 scheme allows preservation of water mass properties, thus preventing spurious convection from occurring.

Although the salinity profiles are generally better reproduced by TOIS than TOI, the sea level variability, measured by the rms errors between the T/P sea surface height and the two model experiments, is not noticeably improved with TOIS. This is mainly because spurious convection in TOI has little impact on sea level as the vertically integrated density is essentially unaltered.

The approach of this paper has been to use in situ thermal data to correct salinity. A similar type of approach, but based on EOFs, has also been tested by Vossepoel et al. (1999), but in their scheme a back history of salinity is used in order to derive the EOFs. This is a serious limitation in applying the scheme in a global assimilation system such as that used at ECMWF. Indeed, one of the regions of improved response of our scheme was shown to be the Atlantic where the mean state was substantially improved. The Atlantic, an area with limited T and S data coverage, was not considered by Vossepoel et al. (1999).

Vossepoel and Behringer (2000) have extended their schemes to include altimetry. This is clearly a next step for us too. The use of altimeter data in the ECMWF system has been explored with encouraging results by Segschneider et al. (2000), and we have recently combined the scheme described here with altimeter data from T/P and the European Remote-Sensing Satellite (ERS). A similar effort has also combined these schemes in the Ocean Circulation and Climate Advanced Modelling Project (OCCAM) high-resolution model (K. Haines 2000, personal communication). One of the main reasons for becoming interested in salinity came from comparing the model sea level with real-time altimeter

data as part of the Developing Use of Altimetry for Climate Studies (DUACS) program of the European Community. This led to a realization that salinity was being handled badly in our real-time analysis system. Therefore, the integration of altimeter information into the system presented here can only improve the performance of our simulations.

Vossepoel and Behringer (2000) have considered using surface salinity observations. A better representation of the sea surface salinity would greatly improve the top 50 m of the vertical salinity profile, as found by Reynolds et al. (1998). However, they also point out that the surface signal is unable to penetrate below this depth. Therefore, the improvement of the upper water column given by the use of surface salinity would complement the TH99 scheme analysis for the remaining part of the water column, so as to provide a better analysis throughout the water column. This is not idle speculation as there is a real prospect that surface salinity observations from satellite will become available in the not-too-distant future (Lagerloef et al. 1995). In addition many of the floats in the Argo network, which is currently being established, will provide salinity profile data which will greatly help in keeping the model T–S relationship on track.

Overall, our results present a method which overcomes many of the troublesome aspects of a univariate OI scheme. It is not, however, a panacea. The concept of T–S conservation is inappropriate in the surface layer, hence sea surface salinity data would greatly help to improve the assimilation scheme. We could perhaps also obtain some improvement in the salinity analysis either by including altimeter data or tuning the assimilation scheme further. However, it seems unlikely that the salinity field will be well reproduced in ocean models without the assimilation of at least some salinity observations from both the surface and the subsurface, at regular intervals.

REFERENCES

Alves, J. O. S., D. L. T. Anderson, T. N. Stockdale, M. A. Balmaseda, and J. Segschneider, 1998: Sensitivity of ENSO forecasts to ocean initial conditions, *Proc. Int. Symp. Triangle'98,* Kyoto, Japan, JAMSTEC, 21–30.

Arakawa, A., and R. V. Lamb, 1977: Computational design of the basic dynamical processes of the UCLA general circulation model. *Methods Comput. Phys.,* **17,** 173–275.

Cooper, N., 1988: The effect of salinity on tropical ocean models. *J. Phys. Oceanogr.,* **18,** 697–707.

Emery, W. J., and L. J. Dewar, 1982: Mean temperature-salinity, salinity-depth and temperature-depth curves in the North Atlantic and North Pacific. *Progress in Oceanography,* Vol. 16, Pergamon, 219–305.

Fischer, M., M. Latif, M. Flugel, and M. Ji, 1997: The impact of data assimilation on ENSO simulations and predictions. *Mon. Wea. Rev.,* **125,** 819–829.

Ji, M., D. W. Behringer, and A. Leetmaa, 1998: An improved coupled model for ENSO prediction and implications for ocean initialization. Part II: The coupled model. *Mon. Wea. Rev.,* **126,** 1022–1034.

——, R. W. Reynolds, and D. W. Behringer, 2000: Use of TOPEX/Poseidon sea level data for ocean analyses and ENSO prediction: Some early results. *J. Climate,* **13,** 216–231.

Kessler, W. S., 1999: Interannual variability of the subsurface high salinity tongue south of the equator at 165°E. *J. Phys. Oceanogr.,* **29,** 2038–2049.

Lagerloef, G. S. E., C. T. Swift, and D. M. L. Vine, 1995: Sea surface salinity: The next remote sensing challenge. *Oceanography,* **8,** 44–50.

Le Traon, P. Y., F. Nadal, and N. Ducet, 1998: An improved mapping method of multisatellite altimeter data. *J. Atmos. Oceanic Technol.,* **15,** 522–534.

Levitus, S., and T. P. Boyer, 1994: *Temperature.* Vol. 4, *World Ocean Atlas 1994,* NOAA Atlas NESDIS, 117 pp.

——, R. Burgett, and T. P. Boyer, 1994: *Salinity.* Vol. 3, *World Ocean Atlas 1994,* NOAA Atlas NESDIS, 99 pp.

Pacanowski, R. C., and S. G. H. Philander, 1981: Parameterization of vertical mixing in numerical models of the tropical oceans. *J. Phys. Oceanogr.,* **11,** 1443–1451.

Reynolds, R. W., and T. M. Smith, 1995: A high resolution global sea surface temperature climatology. *J. Climate,* **8,** 1571–1583.

——, M. Ji, and A. Leetmaa, 1998: Use of salinity to improve ocean modeling. *Phys. Chem. Earth,* **23,** 543–543.

Rosati, A., K. Miyakoda, and R. Gudgel, 1997: The impact of ocean initial conditions on ENSO forecasting with a coupled model. *Mon. Wea. Rev.,* **125,** 754–772.

Segschneider, J., D. L. T. Anderson, and T. N. Stockdale, 2000: Toward the use of altimetry for operational seasonal forecasting. *J. Climate,* **13,** 3115–3138.

Smith, N. R., J. E. Blomley, and G. Meyers, 1991: A univariate statistical interpolation scheme for subsurface thermal analyses in the tropical oceans. *Progress in Oceanography,* Vol. 28, Pergamon, 219–256.

Stockdale, T. N., D. L. T. Anderson, J. O. S. Alves, and M. A. Balmaseda, 1998: Global seasonal rainfall forecasts using a coupled ocean–atmosphere model. *Nature,* **392,** 370–373.

Troccoli, A., and K. Haines, 1999: Use of the temperature–salinity relation in a data assimilation context. *J. Atmos. Oceanic Technol.,* **16,** 2011–2025.

Vossepoel, F. C., and D. W. Behringer, 2000: Impact of sea level assimilation on salinity variability in the western equatorial Pacific. *J. Phys. Oceanogr.,* **30,** 1706–1721.

——, R. W. Reynolds, and L. Miller, 1999: Use of sea level observations to estimate salinity variability in the tropical Pacific. *J. Atmos. Oceanic Technol.,* **16,** 1401–1415.

Wolff, J., E. Maier-Reimer, and S. Legutke, 1997: The Hamburg Ocean Primitive Equation model. Tech. Rep. 13, Deutsches KlimaRechenZentrum, Hamburg, Germany, 98 pp.

Yu, X., and M. McPhaden, 1999: Seasonal variability in the equatorial Pacific. *J. Phys. Oceanogr.* **29,** 925–947.